

Bistable switching in the lossy side-coupled plasmonic waveguide-cavity structures

Xu-Sheng Lin,^{1,2} Jun-Hu Yan,² Yun-Bao Zheng,² Li-Jun Wu,¹ and Sheng Lan^{1,*}

¹Laboratory of Photonic Information Technology, School for Information and Optoelectronic Science and Engineering, South China Normal University, Guangzhou 510006, China

²School of Electronic and Information Engineering, Guangdong Polytechnic Normal University, Guangzhou 510665, China

*slan@scnu.edu.cn

Abstract: We show numerically that the lossy side-coupled plasmonic resonators can be used as bistable switches without compensation. While the internal loss imposes on the bistable characteristics by reducing the transmission contrast and raising the input power requirement, it makes the switching more available by enlarging the width of the hysteresis loop. We also correct the nonlinear transmission formula of the resonators to adapt the lossy condition. Both the theoretical and simulation results are in good agreement.

©2011 Optical Society of America

OCIS codes: (240.6680) Surface plasmons; (190.1450) Bistability; (190.3270) Kerr effect.

References and links

1. H. Raether, *Surface Plasmons on Smooth and Rough Surfaces and on Gratings* (Springer-Verlag, 1987).
2. W. L. Barnes, A. Dereux, and T. W. Ebbesen, "Surface plasmon subwavelength optics," *Nature* **424**(6950), 824–830 (2003).
3. E. Ozbay, "Plasmonics: merging photonics and electronics at nanoscale dimensions," *Science* **311**(5758), 189–193 (2006).
4. M. L. Brongersma and P. G. Kik, *Surface Plasmon Nanophotonics* (Springer, 2007).
5. H. M. Gibbs, *Optical Bistability: Controlling Light with Light* (Academic, 1985).
6. G. A. Wurtz and A. V. Zayats, "Nonlinear surface plasmon polaritonic crystals," *Laser Photonics Rev.* **2**(3), 125–135 (2008).
7. M. Soljačić, M. Ibanescu, S. Johnson, Y. Fink, and J. Joannopoulos, "Optimal bistable switching in nonlinear photonic crystals," *Phys. Rev. E Stat. Nonlin. Soft Matter Phys.* **66**(5), 055601 (2002).
8. M. F. Yanik, S. Fan, and M. Soljačić, "High-contrast all-optical bistable switching in photonic crystal microcavities," *Appl. Phys. Lett.* **83**(14), 2739–2741 (2003).
9. S. Fan, "Sharp asymmetric line shapes in side-coupled waveguide-cavity systems," *Appl. Phys. Lett.* **80**(6), 908–910 (2002).
10. Z. Yu, G. Veronis, S. Fan, and M. L. Brongersma, "Gain-induced switching in metal-dielectric-metal plasmonic waveguides," *Appl. Phys. Lett.* **92**(4), 041117 (2008).
11. C. Min and G. Veronis, "Absorption switches in metal-dielectric-metal plasmonic waveguides," *Opt. Express* **17**(13), 10757–10766 (2009).
12. Y. Shen and G. P. Wang, "Optical bistability in metal gap waveguide nanocavities," *Opt. Express* **16**(12), 8421–8426 (2008).
13. Z. J. Zhong, Y. Xu, S. Lan, Q. F. Dai, and L. J. Wu, "Sharp and asymmetric transmission response in metal-dielectric-metal plasmonic waveguides containing Kerr nonlinear media," *Opt. Express* **18**(1), 79–86 (2010).
14. J. Seidel, S. Grafström, and L. Eng, "Stimulated emission of surface plasmons at the interface between a silver film and an optically pumped dye solution," *Phys. Rev. Lett.* **94**(17), 177401 (2005).
15. M. Nezhad, K. Tetz, and Y. Fainman, "Gain assisted propagation of surface plasmon polaritons on planar metallic waveguides," *Opt. Express* **12**(17), 4072–4079 (2004).
16. G. A. Wurtz, R. Pollard, and A. V. Zayats, "Optical bistability in nonlinear surface-plasmon polaritonic crystals," *Phys. Rev. Lett.* **97**(5), 057402 (2006).
17. C. Min, P. Wang, C. Chen, Y. Deng, Y. Lu, H. Ming, T. Ning, Y. Zhou, and G. Yang, "All-optical switching in subwavelength metallic grating structure containing nonlinear optical materials," *Opt. Lett.* **33**(8), 869–871 (2008).
18. H. Lu, X. Liu, L. Wang, Y. Gong, and D. Mao, "Ultrafast all-optical switching in nanoplasmonic waveguide with Kerr nonlinear resonator," *Opt. Express* **19**(4), 2910–2915 (2011).
19. H. A. Haus, *Wave and Fields in Optoelectronics* (Prentice-Hall, 1984).
20. A. Hosseini and Y. Massoud, "Nanoscale surface plasmon based resonator using rectangular geometry," *Appl. Phys. Lett.* **90**(18), 181102 (2007).

21. T. W. Lee and S. K. Gray, "Subwavelength light bending by metal slit structures," *Opt. Express* **13**(24), 9652–9659 (2005).
 22. Y. Hamanaka, K. Fukuta, A. Nakamura, L. M. Liz-Marzan, and P. Mulvaney, "Enhancement of third-order nonlinear optical susceptibilities in silica capped Au nanoparticle films with very high concentrations," *Appl. Phys. Lett.* **84**(24), 4938–4940 (2004).
 23. J. B. Han, D. J. Chen, S. Ding, H. J. Zhou, Y. B. Han, G. G. Xiong, and Q. Q. Wang, "Plasmon resonant absorption and third-order optical nonlinearity in Ag-Ti cosputtered composite films," *J. Appl. Phys.* **99**(2), 023526 (2006).
 24. J. C. Chen, H. A. Haus, S. Fan, P. R. Villeneuve, and J. D. Joannopoulos, "Optical filters from photonic band gap air bridges," *J. Lightwave Technol.* **14**(11), 2575–2580 (1996).
-

1. Introduction

Nanoplasmonics, a branch of photonics dealing with light in the nano metallic structures, maintained as a hot research field recently [1–4]. People believe that the nanoplasmonic devices have the potential to realize the high density optical circuits and the all-optical communication. To achieve the objectives, one of the important things to do is to investigate the control light with light in the fashion of optical bistability in subwavelength scale [5,6]. For the plasmonic crystals coated with nonlinear polymer whose refractive index being modified by the intensity of control light, bistability of transmission through the structures can be observed for all main plasmonic modes [6]. When we focus on the device model that contains one nonlinear optical resonator, it is found that the coupled waveguide-cavity structures are widely accepted as a promising scheme for optical switching due to the simple configuration and the distinctive physics [7–13]. It has been argued that the side-coupled style is superior to the direct-coupled one because of the accessibility of zero-transmission, which results in an infinite transmission contrast [8]. As regards the plasmonic resonators, however, the internal loss of metal reduces the transmission contrast, especially when the metal gap between the resonator and the waveguide is not narrow enough [10]. Gain media have been introduced to create stimulated emission of surface plasmons and realize lossless propagation in the plasmonic waveguides [14,15]. Thus, they can be filled into the resonator to annul the internal loss and recover the low transmission states [10]. Another proposal involves filling the resonator with active absorption materials, which can lead to very high transmission contrast when the absorption coefficient is tuned by a control light [11]. The switching time, however, is limited by the carrier lifetime, which is on the order of 0.2ns for the gain-assisted switching and 40ns for the absorbing-induced one [10,11]. Therefore, mechanism based on the Kerr nonlinear effect has its clear advantage. The switching time could drop to the order of 1ps or even less [12,16–18].

To date, the studies on the switching of the side-coupled plasmonic resonators are mainly restricted to the use of active media. A natural question is whether the lossy resonators can act as bistable switches without compensation. In this regard, understanding the impacts of the internal loss on the bistable characteristics, such as the maximum transmission contrast, the location and the width of bistable region, etc., should be very helpful. In this Letter, we first characterize the nonlinear transmission of the side-coupled resonators by the numerical simulations using the finite-difference time-domain (FDTD) technique, focusing on the bistability of transmission. Then we explain the simulation results according to the nonlinear transmission formula corrected based on the law of conservation of energy and the coupled mode theory (CMT) [19].

2. FDTD simulation

Consider a silver metal-dielectric-metal (MDM) waveguide side-coupled to a rectangular cavity as shown in the inset of Fig. 1. Such models had been studied by many researchers [10,11,13,20]. We fill the waveguide with silica glass and set the width of waveguide as 50nm so that only the fundamental TM mode could be excited. A Drude-Lorentz function, which provides a good description of empirical dielectric constant data for silver and had been used to calculate the subwavelength light bending [21], is used here to model the permittivity of silver. The rectangular cavity is 300nm long and 300nm wide, filled with some nonlinear composite material with refractive index $n_0 = 1.45$. We set its third-order nonlinear

susceptibility $\chi^{(3)}$ as 2.4×10^{-9} esu, two magnitudes smaller than the recent developed metal-dielectric composite materials [22,23]. In the following simulations, commercial FDTD softwares developed by Rsoft Company are used. The grid size is 2nm for x direction and 5nm for z direction. Also, to avoid any Fabry-Perot resonance effect caused by the waveguide entrances, which may make the transmission spectrum sharp and asymmetric [9,13], the waveguide is truncated before the upper entrance with perfectly matched absorbing layer (PML). The PML conditions are also applied to other boundaries.

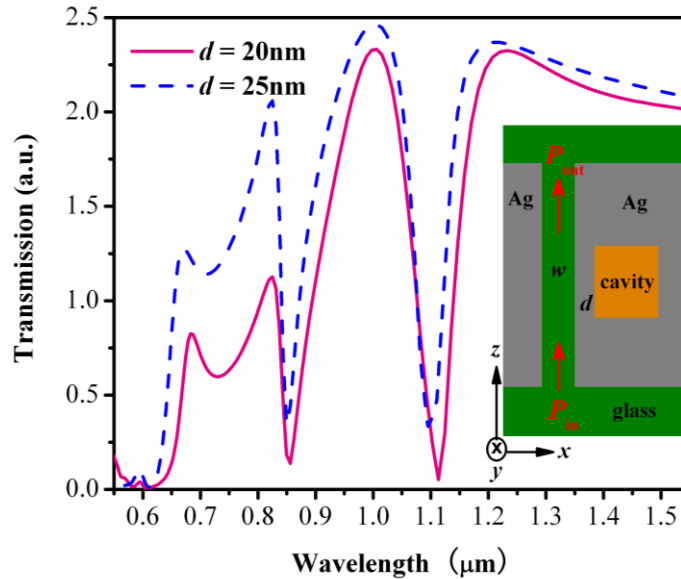


Fig. 1. Transmission spectra of the side coupled plasmonic resonator under the weak nonlinear condition. Inset shows the schematic model studied.

When the interval between the waveguide and the resonator, denoted as d as shown in the inset of Fig. 1, is 20nm, two near-infrared resonances located at $0.855\mu\text{m}$ and $1.115\mu\text{m}$ can be found under the weak launch condition. They are indicated as the solid curve in Fig. 1. We choose the resonance of $\lambda_0 = 1.115\mu\text{m}$ for further investigation because its mode field is nodeless, which can localize more energy and be favor of the Kerr nonlinear effect. By using the method introduced in [24], the decay rate of the cavity field into the waveguide and the rate of internal loss, denoted as γ_e and γ_0 , are measured numerically as $0.137c/\mu\text{m}$ and $0.021c/\mu\text{m}$, respectively, where c is the speed of light in vacuum. So the quality factor of the cavity mode is 17.8.

To search for the bistability, a continue wave (CW) was launched to the lower entrance of the slit waveguide. The carrier wavelength λ is set as $1.20\mu\text{m}$, so the frequency detuning with respect to the resonance, defined as $\delta = 2\pi c(1/\lambda_0 - 1/\lambda)/(\gamma_e + \gamma_0)$, is 2.53. By measuring the transmission $P_{\text{out}}/P_{\text{in}}$, where P_{in} and P_{out} represent the input and stable output powers of the CW, respectively, we obtain the upper branch of hysteresis depicted as the open down-triangles in Fig. 2(a). Here, to eliminate the loss effect of the slit waveguide, the results are normalized to the transmission of the same isolated waveguide. When P_{in} is small, the resonance shifts hardly so little energy couples into the cavity. It leads to the high transmission states that make up of the upper branch of hysteresis. A dramatic drop of transmission from 0.74 to 0.17 occurs when P_{in} increases a little from $5.90\text{W}/\mu\text{m}$ to $5.95\text{W}/\mu\text{m}$, as the right dotted line shown in Fig. 2(a), indicating that the accumulated energy in the resonator has become large enough to create a decay wave that interferences almost destructively with the input wave. Then it grows linearly with P_{in} because the energy in the resonator has reached its maximum, i.e., the resonant frequency has caught the CW frequency.

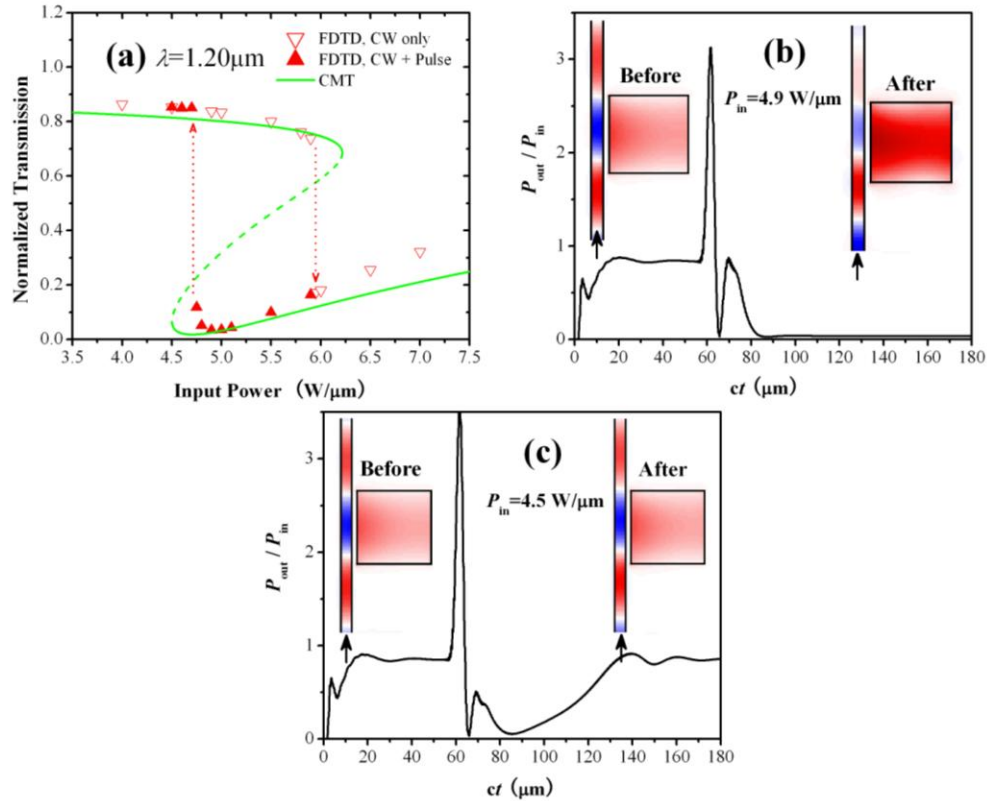


Fig. 2. (a) Hysteresis loop when the interval between the waveguide and cavity is 20 nm. (b) and (c) show the transmission as a function of time when P_{in} is $4.9 W/\mu m$ and $4.5 W/\mu m$, respectively. Insets are the snapshots of the electric fields corresponding to the stable outputs before and after the Gaussian pulse, where red and blue represent the positive and negative fields. All panels use the same color scale. Arrows mark the CW launch direction.

The lower branch of hysteresis can be accessed by superposing the CW input with a high peak-power Gaussian pulse, which drags the transmission from its upper state to the lower one if it has [8]. Two typical processes corresponding to $P_{in} = 4.90 W/\mu m$ and $4.50 W/\mu m$ are recorded in Figs. 2(b) and 2(c), respectively. They show the ratio P_{out}/P_{in} as a function of ct , the speed of light in vacuum multiplied by time. The Gaussian pulse (width = $10.3 fs$, peak power = $500 W/\mu m$) is launched when $ct = 47 \mu m$, the time when the output is stable. For the case of $4.90 W/\mu m$, the transmission can be switched from 0.84 to 0.03 by the pulse as the panel shows. There exists a lower transmission state that corresponds to very strong cavity field. On contrast, when $P_{in} = 4.50 W/\mu m$, the transmission rests on 0.85, the stable value before the pulse, and the cavity field varies little, meaning no existence of the lower transmission state. In this way, we can find out all the states of the lower branch shown as the closed up-triangles and determine the bistable region, which is the space between the two dotted lines in Fig. 2(a). We find that the maximum transmission contrast is 28 which corresponds to $P_{in} = 4.90 W/\mu m$. The width of hysteresis loop, defined as the value space of P_{in} when bistability is available, can be measured as $1.15 W/\mu m$. Obviously, this lossy resonator can act as a bistable switch.

We increase the interval d from 20 nm to 25 nm to see if any improvements in bistability could be achieved. The resonance shifts a little and locates at $1.095 \mu m$ as the dashed curve shown in Fig. 1. The decay rate of the cavity field into the waveguide and the rate of internal loss can be measured as $0.120 c/\mu m$ and $0.063 c/\mu m$, respectively, so the quality factor of the cavity mode is 15.7. Similar to the above process, we can plot the hysteresis loop of

transmission when the CW wavelength is $1.20\mu\text{m}$ in Fig. 3. The maximum transmission contrast is about 13, which corresponds to $P_{\text{in}} = 5.6 \text{ W}/\mu\text{m}$. It is much smaller than 28, the case of 20nm , due to the increase of minimum transmission. Surprisingly, the width of hysteresis loop can be measured as $3.3\text{W}/\mu\text{m}$, almost three times as much as the previous case. As here the frequency detuning and the quality factor are only a little difference from the case of $d = 20\text{nm}$, it should be impossible to cause such a width of hysteresis loop. We guess that it originates from the obvious difference of the internal loss, which are $0.021\text{c}/\mu\text{m}$ and $0.063\text{c}/\mu\text{m}$, respectively.

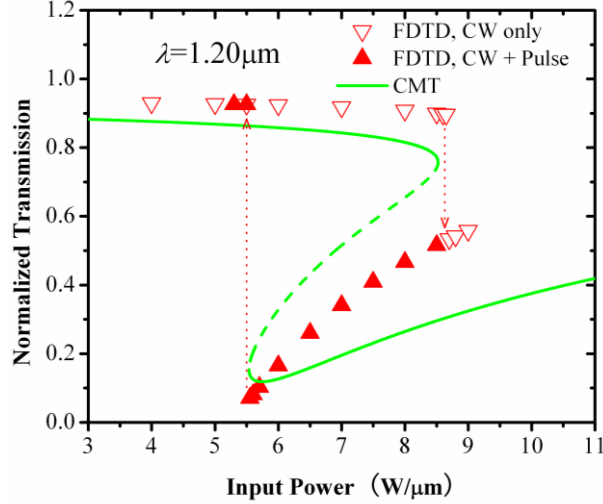


Fig. 3. Hysteresis loop when the interval between the waveguide and cavity is 25 nm .

3. CMT analysis

We explain the simulation results by using the corrected nonlinear transmission formula. According to CMT and the perturbation theory, the transmission of side coupled resonator when the internal loss is negligible can be written as [8]

$$T = \frac{P_{\text{out}}}{P_{\text{in}}} = \frac{\left(\frac{P_{\text{ref}}}{P_0} - \delta\right)^2}{\left(\frac{P_{\text{ref}}}{P_0} - \delta\right)^2 + 1} = \frac{\left(\frac{P_{\text{in}} - P_{\text{out}}}{P_0} - \delta\right)^2}{\left(\frac{P_{\text{in}} - P_{\text{out}}}{P_0} - \delta\right)^2 + 1}, \quad (1)$$

where P_0 is the nonlinear characteristic power reflecting the nonlinear feedback and power confinement of the resonator [7,8], P_{in} , P_{ref} , and P_{out} are respectively the input, reflected, and output powers in the coupled waveguide. Equation (1) should be corrected when the internal loss is taken into account. First, the minimum transmission, which is zero according to Eq. (1), must be replaced by $\eta_0 = [\gamma_0/(\gamma_0 + \gamma_c)]^2$ if we use the result from CMT [10,19]. Due to the non-zero η_0 , the infinite transmission contrast decreases to about $1/\eta_0$, as shown by the above simulation results. Second, the relation $P_{\text{in}} - P_{\text{out}} = P_{\text{ref}}$ is no longer valid under the lossy condition. Instead, we have $P_{\text{in}} - P_{\text{out}} = P_{\text{ref}} + P_{\text{lossy}}$ according to the law of conservation of energy, where P_{lossy} is the power of internal loss. It can be expressed as $P_{\text{lossy}} = 2\gamma_0 E$ where E is the stored energy in the resonator. Also, $P_{\text{ref}} = \gamma_c E$ if the decay rates of E along the two directions of the slit waveguide (upwards and downwards in our model) are equal. In this way, we can obtain the expression

$$P_{\text{in}} - P_{\text{out}} = P_{\text{ref}} (1 + 2\alpha), \quad (2)$$

where α defined as (γ_0/γ_e) , the energy loss with respect to that couples into the waveguide. Thus, under the nonlinear lossy condition, Eq. (1) must be corrected as

$$T = \frac{P_{\text{out}}}{P_{\text{in}}} = \frac{\left[\frac{P_{\text{in}} - P_{\text{out}}}{(1 + 2\alpha)P_0} - \delta \right]^2 + \eta_0}{\left[\frac{P_{\text{in}} - P_{\text{out}}}{(1 + 2\alpha)P_0} - \delta \right]^2 + 1}. \quad (3)$$

Based on Eq. (3), we can see that it is the factor $(1 + 2\alpha)$ that widens the hysteresis loop. As α is much larger when $d = 25\text{nm}$, the corresponding hysteresis loop is naturally much wider, as shown by the simulation result in Fig. 3. Based on Eq. (3), we also give the theoretical bistable curves in Figs. 2(a) and 3 where the solid lines and the dashed lines represent the stable and unstable states, respectively. For the case of $d = 20\text{nm}$, which shown in Fig. 2(a), the theory predicts correctly most of the bistable states, but the width of hysteresis loop is wider than the simulation result. For the case of $d = 25\text{nm}$, however, the theoretical width of hysteresis loop is in good agreement with the simulation one, while the value of transmission shows an obvious discrepancy, as shown in Fig. 3. As a whole, Eq. (2) expresses the bistable characteristics of the lossy resonators quite well.

4. Conclusion

The internal loss of metals has serious impacts on the bistable characteristics of the plasmonic resonators. It raises the input power requirement, reduces the transmission contrast and widens the width of bistable region. Such phenomena can be explained by using the corrected formula based on the law of conservation of energy and the coupled mode theory. Even the resonator is filled with Kerr nonlinear material without compensation, the transmission contrast of optical bistability is still high enough for practical applications.

Acknowledgments

The authors acknowledge the financial support from the National Natural Science Foundation of China (NSFC) (Grant Nos. 60778032 and 10974060).